Contribution of Structural Peculiarities of Onconase to Its High Stability and Folding Kinetics†

Ulrich Arnold,* Cindy Schulenburg, Doreen Schmidt, and Renate Ulbrich-Hofmann

Department of Biochemistry/Biotechnology, Martin-Luther University Halle-Wittenberg, Kurt-Mothes Strasse 3, 06120 Halle, Germany

Received December 10, 2005; Revised Manuscript Received February 2, 2006

ABSTRACT: Onconase (ONC) from *Rana pipiens* is the smallest member of the ribonuclease A (RNase A) superfamily. Despite a tertiary structure similar to RNase A, ONC is distinguished by an extremely high thermodynamic stability. In the present paper we have probed the significance of three structural regions, which exhibit structural peculiarities in comparison to RNase A, for the stability of ONC to temperature and guanidine hydrochloride induced denaturation: (i) the N-terminal pyroglutamate residue, (ii) the hydrophobic cluster between helix I and the first β-sheet, and (iii) the C-terminal disulfide bond. For this purpose, the enzyme variants <E1E-, <E1P-, F28T-, F28A-, F36Y-, and C87A/C104A-ONC were produced and studied in equilibrium and kinetic measurements. The destabilizing influence of the mutations strongly depended on the modified structural region. The exchanges of the N-terminal pyroglutamate (<E1E- and <E1P-ONC) had the smallest impact ($\Delta\Delta G^{[D]_{50\%}} = 4.2$ and 7.0 kJ mol^{-1}), while interferences in the hydrophobic cluster (F28T-, F28A-, and F36Y-ONC) had larger effects ($\Delta\Delta G^{[D]_{50\%}} = 22.2$, 20.9, and 19.5 kJ mol^{-1}). The removal of the C-terminal disulfide bond (C87A/C104A-ONC) showed the largest influence on stability ($\Delta\Delta G^{[D]_{50\%}} = 32.0$ kJ mol^{-1}). As concluded from the comparison of $\Delta\Delta G^{[D]_{50\%}}$ and $\Delta\Delta G_U^{\ddagger[D]_{50\%}}$, all destabilization effects were exclusively caused by increased unfolding rate constants except for C87A/C104A-ONC, where unfolding as well as folding was impacted. Of all amino acid residues investigated, Phe28, which is unique for ONC among the ribonucleases, had the greatest importance for rate of unfolding. Our data on the folding and unfolding kinetics indicate that the strong stabilization of ONC in comparison to RNase A is caused by a dramatic deceleration of the unfolding reaction.

Onconase (ONC;[1] Alfacell Corp., Bloomfield, NJ), which is also known as P-30 protein or ranpirnase, is a ribonuclease from oocytes or early embryos of the Northern leopard frog *Rana pipiens*. The discovery of the anticancer effects of this protein (*1*) made ONC a promising antitumor therapeutic, and it has reached phase III clinical trials (*2*). On the basis of its three-dimensional structure (Figure 1), ONC belongs to the ribonuclease A (RNase A) superfamily despite a sequence identity of only 30% with RNase A. With a melting temperature of 90 °C (*3*), however, its thermal stability exceeds that of most members by about 30 K. Even though various "rules" for protein stabilization have been elucidated (*4*, *5*), it is not yet fully understood how the concur of the forces finally stabilizes the natively folded protein structure (*6*). The analysis of the differences of structurally highly homologous proteins provides insight into the structural determinants for increased protein stability.

ONC and RNase A share a very similar overall topology (*7*). Particularly, the position of the three α-helices, the β-sheet system, the active site residues, the hydrophobic clusters (*8*), and three out of four disulfide bonds are superimposable. The most obvious structural differences between ONC and RNase A occur in the length and composition of the loop regions and at the chain termini: the N-terminal pyroglutamate residue of ONC, which tethers

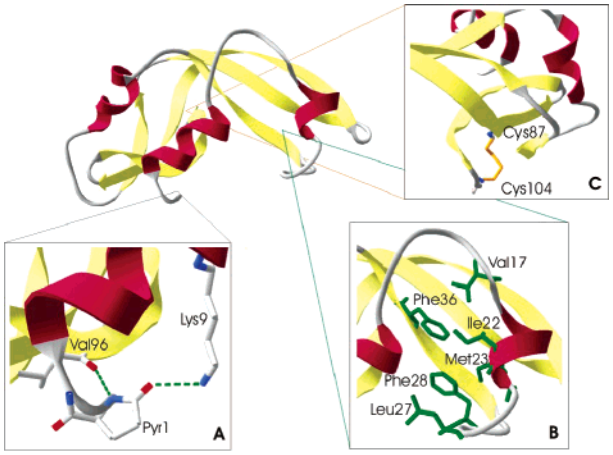

FIGURE 1: Tertiary structure of onconase. The model (1ONC) was taken from the Brookhaven Protein Data Bank and drawn with Swiss pdb-Viewer v3.7. The structural regions for amino acid substitutions are (A) the N-terminal pyroglutamate with hydrogen bonds to Lys9 and Val96, (B) the hydrophobic cluster formed by Val17, Ile22, Met23, Leu27, Phe28, and Phe36, and (C) the C-terminal β-sheet with the disulfide bond Cys87−Cys104.

† This study was supported by the Land Sachsen-Anhalt (3537C/0903L).

* To whom correspondence should be addressed. E-mail: ulrich.arnold@biochemtech.uni-halle.de. Phone: +49 345 5524865. Fax: +49 345 5527303.

[1] Abbreviations: CD, circular dichroism; DSC, differential scanning calorimetry; GdnHCl, guanidine hydrochloride; ONC, onconase; RNase, ribonuclease.

10.1021/bi0525223 CCC: $33.50
Published on Web 02/28/2006

the N-terminus to the protein body, and a C-terminal disulfide bond, both of which contribute to the stability of the ONC molecule (*9*−*11*). Additionally, the hydrophobic cluster which is formed by Val17, Ile22, Met23, Leu27, and Phe36 in ONC (corresponding to Tyr25, Met29, Met30, Leu35, and Phe46 in RNase A) is extended by replacing Thr36 in RNase A with Phe28 in ONC (*12*, *13*). While the breakup of the N-terminal pyroglutamyl bond resulted in a decrease of the catalytic activity (*14*, *15*), the thermal stability was only slightly affected (*11*, *16*). In contrast, the deletion of the C-terminal disulfide bond had been shown to dramatically decrease the thermodynamic stability without affecting the catalytic activity to an equal extent (*9*, *10*).

While the thermodynamic stability of ONC and several mutant enzymes thereof has been determined, there are no data on the folding of ONC. The enormous increase in the thermodynamic stability of the ONC molecule in comparison to the other members of the RNase A superfamily by about 20 kJ mol^{-1} (*17*) should be reflected in remarkable changes of the rate constants of the folding and/or unfolding reactions. In the present paper, we have analyzed the effect of amino acid substitutions in three different critical structural regions on the thermodynamic stability as well as on the folding/unfolding kinetics of the ONC molecule. Our results disclose that the stabilization of the ONC molecule in comparison to RNase A is caused by a pronounced deceleration of the unfolding reaction.

MATERIALS AND METHODS

Materials. Restriction enzymes *Hin*dIII, *Nde*I, and *Sap*I and the plasmid pTXB1 were from New England Biolabs, Frankfurt/Main, Germany. Oligonucleotides were from MWG Biotech, Ebersberg, Germany, and the plasmid pET-26b(+) was from Novagen, Bad Soden, Germany. The pET-22b(+) plasmids carrying the gene for wild-type (wt) ONC (*3*) or C87A/C104A-ONC (*10*) were a gift from Prof. R. T. Raines, University of Wisconsin—Madison, WI. Growth media were from Difco Laboratories, Detroit, MI. Yeast RNA was from Sigma, Steinheim, Germany. *Escherichia coli* (*E. coli*) strains XL-1 Blue and BL21(DE3) were from Stratagene, Heidelberg, Germany. *E. coli* strain ER2566 was from New England Biolabs. All other chemicals were of the purest grade commercially available.

Site-Directed Mutagenesis. The *onc* gene was cloned from the plasmid pET-22b(+) into the plasmid pET-26b(+) by standard methods using the PCR and the restriction sites for *Nde*I and *Hin*dIII. Subsequently, the *onc* gene was modified by use of the QuikChange site-directed mutagenesis kit (Stratagene) to obtain the mutations <E1E, <E1P, F28T, F28A, and F36Y. For the expression of <E1P-ONC, two further constructs were created. First, by standard methods of PCR, the <E1P-*onc* gene lacking the pelB leader sequence was amplified and cloned back into the plasmid pET-26b-(+) by the use of the restriction sites for *Nde*I and *Hin*dIII. Second, by use of the restriction sites for *Nde*I and *Sap*I, the <E1P-*onc* gene was cloned into the plasmid pTXB1. In contrast to the other constructs, these two constructs lack the DNA sequence for the expression of the pelB signal sequence but carry the trinucleotide AUG for the additional start methionine in front of the <E1P-*onc* gene. The mutations were verified by DNA sequencing according to Sanger et al. (*18*) using the SequiThermExcel LongRead DNA sequencing kit (Biozym, Hess. Oldendorf, Germany) and a Li-COR 4000 DNA sequencer (MWG Biotech).

Expression, Renaturation, and Purification of the Enzyme Variants. The experimental procedures were performed as described previously (*19*) except for the expression of the variant <E1P-ONC in pTXB1, which was performed according to ref *20* (see below). Briefly, cultures of *E. coli* strain BL21(DE3) that had been transformed with a plasmid directing the expression of the corresponding ONC variant were grown in terrific broth containing 50 μg mL^{-1} kanamycin [wt-ONC and the variants <E1E, <E1P, F28A, F28T, and F36Y in vector pET-26b(+)] or 100 μg mL^{-1} ampicillin [C87A/C104A-ONC in vector pET-22b(+)] at 37 °C to an OD_{600nm} of 2. Gene expression was induced by 1 mM isopropyl β-D-thiogalactopyranoside, and cells were grown for an additional 4 h before being harvested. Cell lysis was performed by treatment with lysozyme and homogenization with a Gaulin homogenizer. The inclusion bodies were isolated by centrifugation followed by resolubilization (20 mM Tris-HCl, 6 M GdnHCl, 250 mM dithiothreitol, 10 mM EDTA, pH 8.0) and dialysis of the protein solution against 20 mM acetic acid. Precipitates formed during dialysis were removed by centrifugation. After renaturation in 100 mM Tris-HCl, 100 mM NaCl, 10 mM EDTA, and 1 mM reduced and 0.2 mM oxidized glutathione, pH 8.0, at room temperature for 36 h, the protein was purified on a SOURCE S column (Amersham Biosciences, 50 mM Tris-HCl, pH 7.5, with a linear gradient of 0−500 mM NaCl). Cyclization of the N-terminal glutamine residue (in wt-ONC and the variants F28T, F28A, F36Y, and C87A/C104A) was achieved by dialysis of the purified proteins against 200 mM sodium phosphate buffer, pH 7.0, for 3 days at room temperature.

E. coli ER2566 cells that had been transformed with a plasmid directing the expression of <E1P-ONC fused to the *mxe*-intein (<E1P-*onc* in plasmid pTXB1) were cultivated in Luria−Bertani medium containing ampicillin (100 μg mL^{-1}) with shaking at 37 °C until $OD_{600nm} = 0.5$. Gene expression was then induced by the addition of isopropyl β-D-thiogalactopyranoside (0.5 mM), and the cultures were grown for an additional 3−4 h at 25 °C. Cell lysis by sonication, affinity chromatography of the soluble material on chitin beads, and cleavage by a buffer containing dithiothreitol (50 mM) were carried out according to the instructions of the manufacturer (New England Biolabs). For the elution of the cleavage product (<E1P-ONC) 3 M GdnHCl had to be applied. Dialysis, renaturation, and purification were performed as described above.

Determination of the Protein Concentration. The protein concentration was determined using an absorption coefficient of $\epsilon = 0.87$ mL mg^{-1} cm^{-1} at 280 nm (*3*) except for F36Y-ONC where an absorption coefficient of $\epsilon = 1.0$ mL mg^{-1} cm^{-1} at 280 nm calculated according to Pace et al. (*21*) was used.

Mass Spectrometry. Protein samples were desalted by use of ZipTip pipet tips (Millipore, Schwalbach, Germany). Determination of molecular masses was performed by electrospray ionization (Esquire) or matrix-assisted laser desorption ionization mass spectrometry (Reflex; Bruker-Franzen, Bremen, Germany).

Activity. Ribonucleolytic activity of ONC and its variants was determined with yeast RNA as substrate following the

procedure by Corbishley et al. (*22*). All solutions were prepared with diethyl pyrocarbonate-treated water. Yeast RNA was dissolved in 100 mM sodium acetate buffer, pH 5.5, followed by addition of 3 volumes of ice-cold ethanol and centrifugation (20000*g*, 4 °C, 15 min) to remove soluble oligonucleotides. The dried RNA pellet was dissolved in 100 mM sodium acetate buffer, pH 5.5, and the concentration of the RNA was determined spectrophotometrically [$E_{260} = 1$ corresponds to 40 μg mL^{-1} RNA (*23*)]. The concentration of wt-ONC and its variants in the reaction mixtures of 250 μL was 0.7 μg mL^{-1}, and the concentration of RNA was 2.8 mg mL^{-1}. After incubation at 37 °C for 15 min the reaction was stopped by addition of 250 μL of 22 mM $LaCl_3$ in 1.2 M perchloric acid. After incubation on ice for 20 min the samples were centrifuged (20000*g*, 4 °C, 20 min). The supernatant was diluted four times with water, and the concentration of soluble nucleotides was determined from the absorbance at 260 nm [$\epsilon_{260nm} = 10600$ M^{-1} cm^{-1} (*24*)]. One unit corresponds to the release of 1 μmol of soluble ribonucleotides/h. Concentrations of enzymes and RNA were chosen in a way to ensure a linear increase of the absorbance with incubation time.

Circular Dichroism (CD) Spectroscopy. CD spectra of wt-ONC and its variants were recorded in 50 mM sodium acetate buffer, pH 5.5, containing 1 mg mL^{-1} protein on a CD spectrometer J-810 (Jasco, Gross-Umstadt, Germany) at 20 °C. Cuvettes of 1 and 0.01 cm path length were used for CD spectroscopy in the near-UV region (250−340 nm) and in the far-UV region (190−260 nm), respectively.

GdnHCl-Induced Transition Curves and Determination of the Parameters of the Thermodynamic Stability. GdnHCl-induced transition curves of wt-ONC and its variants were obtained by fluorescence spectroscopy on a Fluoro-Max-2 spectrometer (Jobin Yvon, Bensheim, Germany) at 25 °C using a cuvette of 1.0 cm × 0.4 cm. Protein concentration was 20 μg mL^{-1} in 100 mM sodium acetate buffer, pH 5.5, containing 0−7.4 M GdnHCl. After equilibration, five fluorescence spectra which were recorded from 305 to 380 nm were averaged. The bandwidth was 1 nm for excitation at 295 and 10 nm for emission.

From the fluorescence spectra, the shift of the wavelength of the emission maximum (y) was determined as a function of the GdnHCl concentration and evaluated by nonlinear regression using the program Sigma Plot according to Santoro and Bolen (*25*) with the modification by Clarke and Fersht (*26*)

$$\Delta G^{[D]} = m_{\Delta G}([D]_{50\%} - [D]) \quad (1)$$

with $[D]_{50\%}$, the concentration of denaturant [D] at which 50% of the protein is denatured, $m_{\Delta G}$, the measure of the dependence of the standard free energy on denaturant concentration, and $\Delta G^{[D]}$, the standard free energy at a given concentration of denaturant, leading to the equation

$$y = \{(y_N^0 + m_N[D]) + (y_D^0 + m_D[D]) \exp(-m_{\Delta G}([D]_{50\%} - [D])/RT)\}/\{1 + \exp(-m_{\Delta G}([D]_{50\%} - [D]/RT)\} \quad (2)$$

where y_N^0 and y_D^0 are the intercepts and m_N and m_D the slopes in the pre- and posttransition region, respectively, in the y vs [D] graph. The fraction of native protein (f_N) was calculated from the fitted values using the equation

$$f_N = (y_D - y)/(y_D - y_N) \quad (3)$$

with

$$y_D = y_D^0 + m_D[D]$$

and

$$y_N = y_N^0 + m_N[D]$$

where y_N and y_D are the signals of the native and the denatured protein as a function of the denaturant concentration. To calculate values of the standard free energy, the linear function

$$\Delta G^{[D]} = \Delta G^{H_2O} - m_{\Delta G}[D] \quad (4)$$

was used where ΔG^{H_2O} is the standard free energy of unfolding in the absence of denaturant (*27*).

Folding Measurements. All experiments were performed in 100 mM sodium acetate buffer, pH 5.5, at 20 °C on a Fluoro-Max-2 spectrometer (Jobin Yvon). Protein samples were preincubated in 0 or 6 M GdnHCl at 20 °C. Unfolding and refolding were initiated by manual addition of GdnHCl solution or buffer to yield the respective final GdnHCl concentration. The final protein concentration was 50 μg mL^{-1}. The bandwidth was 5 nm for excitation at 295 nm and 5 nm for emission at 310, 320, and 358 nm. The observed rate constants (k_{obs}) which are the sum of the rate constants of the respective unfolding reaction (k_U) and refolding reaction (k_f) were calculated from the change of the intensity of the emission signal as a function of time which followed first-order kinetics. The data in the resulting chevron plot (ln k_{obs} vs [D]) were fitted according to Maxwell et al. (*28*)

$$\ln k_{obs} = \ln\left[\exp\frac{\ln k_f^0 + m_f[D]}{RT} + \exp\frac{\ln k_U^0 + m_U[D]}{RT}\right] \quad (5)$$

where k_f^0 and k_U^0 are the rate constants of the folding and unfolding reaction in the absence of denaturant, m_f and m_U are the slopes of the folding and unfolding limbs, and R is the gas constant. On the basis of the Eyring equation

$$\Delta G^{\ddagger} = RT[\ln(K/h) - \ln(k/T)] \quad (6)$$

where $\Delta G^{\ddagger}$, K, h, and R are the free energy of activation, Boltzmann's, Planck's, and the gas constants and k is k_U or k_f at the respective concentration of denaturant, values of $\Delta G^{\ddagger}$ were calculated for the folding or unfolding reaction.

Thermal Stability. Values of the temperature at the transition midpoint T_m were determined by differential scanning calorimetry (DSC). Calorimetric measurements were carried out on a VP-DSC microcalorimeter (MicroCal, Northampton, MA) at a scan rate of 1.5 K min^{-1}. The evaluation of the data and calculations were performed using the program Origin 7.0. Protein solutions were dialyzed against 100 mM sodium acetate buffer, pH 5.5, at 4 °C for at least 12 h, and the protein concentration was determined as described above. Before DSC measurements, the protein

samples were degassed for 5 min (ThermoVac; MicroCal). The excess heat capacity function (ΔC_p) was obtained after baseline correction for the respective buffer system. The enthalpy ΔH was determined by direct integration of the peak area, and T_m corresponds to the maximum of the DSC curve.

SDS−PAGE. Electrophoresis was carried out on a Midget electrophoresis unit (Hoefer, San Francisco, CA) according to Laemmli (*29*) using 10% and 17.5% acrylamide for stacking and separating gels, respectively. The gels were stained with Coomassie Brilliant Blue R250 or with silver nitrate.

RESULTS

Design of the ONC Variants. ONC variants were designed to probe the influence of three structural elements discriminating ONC from RNase A.

(i) The N-Terminus. The N-terminal pyroglutamate in native ONC (Figure 1A), which is formed by cyclization of a glutamine residue, can also be considered as 5-oxoproline. The oxo group forms a hydrogen bond to the side chain of Lys9 which tethers the N-terminus to the protein body and aligns the side chain for proper substrate binding (*7*). We replaced the glutamine residue by proline (<E1P-ONC) to eliminate the oxo group while maintaining the cyclic structure or by glutamate (<E1E-ONC) to disrupt the cyclic structure while maintaining the hydrogen bond to Lys9.

(ii) The Hydrophobic Cluster around Phe36. Concerning the hydrophobic cluster (Figure 1B), we replaced the unique Phe28 of ONC by alanine (F28A-ONC) or by threonine (F28T-ONC), which is the residue present in most members of the RNase A superfamily. Furthermore, we replaced the highly conserved Phe36 by tyrosine (F36Y-ONC). This region which links helix II and the first β-sheet and which contains a hydrophobic cluster had been proposed as the first unfolding region in RNase A (*13*, *30*) because mutations in this region had affected the unfolding reaction only.

(iii) The C-Terminus. The C-terminus of ONC is anchored to the protein body by a disulfide bond (Figure 1C) which occurs only in the amphibian RNases. Because the C-terminal region of RNase A had been proposed as the folding nucleus (*31*), the covalent attachment of the C-terminus to the protein body of ONC was expected to mainly affect the folding reaction. We used an ONC variant in which both cysteines had been replaced by alanine residues (C87A/C104A-ONC) to evaluate the contribution of this disulfide bond to the stability and folding of the ONC molecule.

Expression, Renaturation, and Purification. wt-ONC and all variants except E1P-ONC were expressed as inclusion bodies (*3*), renatured, and purified as described in Materials and Methods. Mass spectrometry proved that the pelB signal sequence had completely been removed (Table 1). In contrast, the expression of the variant <E1P-ONC by the same method failed. Mass spectrometry revealed a mixture of products in the inclusion body material carrying the pelB signal sequence, which had been proteolytically degraded to varying extents (not shown). Thus, two alternative approaches to yield <E1P-ONC were examined. The expression as a fusion protein with the *mxe* intein/chitin binding domain (in plasmid pTXB1) resulted in large part in insoluble material. After thiol-induced cleavage of the soluble protein and purification, about 0.5 mg of protein/L of culture could be obtained. In the second route, <E1P-ONC was expressed as Met(−1)-<E1P-ONC in the plasmid pET-26b(+) without the pelB signal sequence. The resulting inclusion bodies, however, exclusively contained <E1P-ONC without the additional N-terminal Met residue (Table 1) and yielded 20−30 mg mL^{-1} protein/L of culture.

Table 1: Activity, Molecular Mass, and Thermal Stability of wt-Onconase and Its Variants[a]

ONC variant	relative activity (%)	molecular mass (Da): calcd from sequence	molecular mass (Da): determined by mass spectrometry	T_m (°C)
wt-ONC	100 ± 4	11819.7	11819.6	88.5 ± 0.1
<E1E-ONC	41 ± 4	11837.6	11836.8	87.0 ± 0.1
<E1P-ONC[b]	44 ± 8	11805.6	11805.0	87.7 ± 0.2
F28T-ONC	60 ± 4	11773.5	11772.0	77.4 ± 0.2
F28A-ONC	61 ± 7	11743.5	11742.7	78.1 ± 0.2
F36Y-ONC	80 ± 2	11835.7	11834.8	79.2 ± 0.3
C87A/C104A-ONC	66 ± 3	11757.5	11761.2	69.4 ± 0.1

[a] Activity was determined with yeast RNA as substrate at 37 °C as described in Materials and Methods. Values of T_m at pH 5.5 were determined by DSC as described in Materials and Methods. [b] Product of the expression of Met(−1)-<E1P-ONC in the plasmid pET-26b(+).

Even though differing in their tendency to form aggregates during renaturation, all variants could be obtained in sufficient amounts (up to 30 mg L^{-1} of culture medium). The purified proteins proved to be homogeneous by SDS−PAGE and rechromatography on a SOURCE S column.

Activity. The relative activity of the ONC variants, determined with yeast RNA as substrate, revealed that all ONC variants were active (Table 1). As expected from the disturbance of the hydrogen bond to Lys9 and, thus, of the substrate binding, the variants concerning the N-terminus showed the lowest activity.

CD Spectra. As deduced from the CD spectra in the near- and far-UV region, all ONC variants revealed a tertiary and secondary structure comparable to that of wt-ONC (Figure 2). The slightly increased signal in the near-UV region of F36Y-ONC (around 284 nm) can be explained by the introduction of the additional tyrosine. For the C87A/C104A-ONC variant, a slight increase of the signal in both the 208−220 nm and the 250−270 nm region was detected. The increase of the signal in the far-UV region had been reported previously (*10*). The change in the near-UV region is attributed to changes of spectroscopic properties of this variant due to the loss of the disulfide bond but not to changes of structural properties because the signals for the tyrosines (around 284 nm) and the tryptophan (around 291 nm) remain unchanged.

Temperature-Induced Denaturation. The thermal stability of wt-ONC and its variants was investigated by DSC measurements. Thermal unfolding proved to be reversible as judged by reheating experiments and follows a two-state transition model as judged from the fit of the data. In contrast to the activity measurements, replacement of Pyr1 by proline or glutamate had the smallest effect on T_m at pH 5.5 (Table 1). The midpoint of the thermally induced transition decreased by about 10 K as a result of amino acid substitutions in the hydrophobic cluster. However, replacement of the unique Phe28 by Thr or Ala led to a slightly larger decrease in T_m than the substitution of Phe36 by Tyr. The elimination

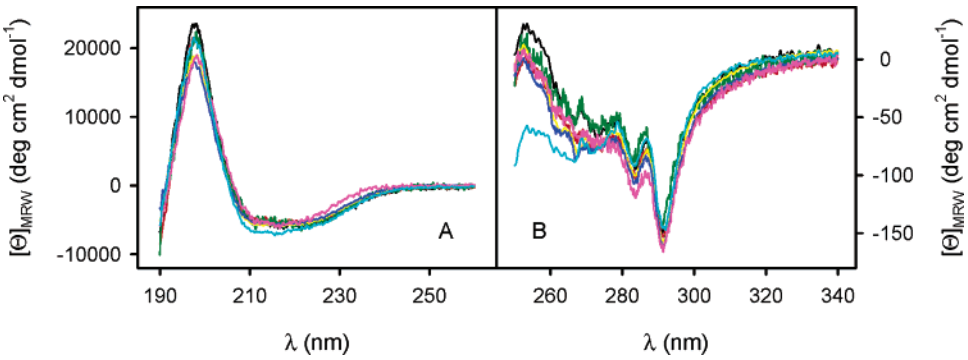

FIGURE 2: Far-UV (A) and near-UV (B) CD spectra of wt-ONC and its variants. CD spectra of wt-ONC (black) and its variants <E1E (red), <E1P (green), F28T (yellow), F28A (dark blue), F36Y (magenta), and C87A/C104A (light blue) were recorded in 50 mM sodium acetate buffer, pH 5.5, at 20 °C using a protein concentration of 1 mg mL^{-1} as described in Materials and Methods.

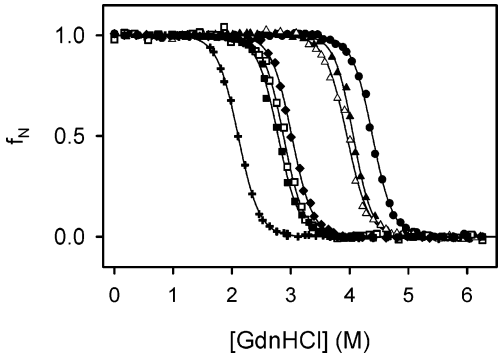

FIGURE 3: GdnHCl-induced transition curves. The transition curves of wt-ONC (●), <E1E (▲), <E1P (△), F28T (■), F28A (□), F36Y (◆), and C87A/C104A (+) were determined by fluorescence spectroscopy in 100 mM sodium acetate buffer, pH 5.5, at 20 °C as described in Materials and Methods.

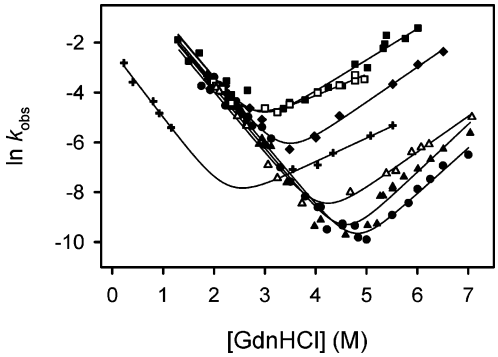

FIGURE 4: Chevron plots for the unfolding and refolding of wt-ONC and its variants. Values of k_{obs} of wt-ONC (●) and its variants <E1E (▲), <E1P (△), F28T (■), F28A (□), F36Y (◆), and C87A/C104A (+) were determined by fluorescence spectroscopy in 100 mM sodium acetate buffer, pH 5.5, at 20.0 °C as described in Materials and Methods.

Table 2: Parameters of Thermodynamic Stability and Unfolding of wt-Onconase and Its Variants[a]

ONC variant	$[D]_{50\%}$	$\Delta\Delta G^{[D]_{50\%}}$ (kJ mol^{-1})	k_U^0 (s^{-1})	$\Delta\Delta G_U^{\ddagger[D]_{50\%}}$ (kJ mol^{-1})
wt-ONC	4.4 ± 0.1		5.44×10^{-9}	
<E1E-ONC	4.1 ± 0.1	4.2	7.72×10^{-9}	1.7
<E1P-ONC	3.9 ± 0.2	7.0	3.17×10^{-7}	6.1
F28T-ONC	2.8 ± 0.1	22.2	1.30×10^{-4}	20.6
F28A-ONC	2.9 ± 0.1	20.9	5.07×10^{-4}	21.1
F36Y-ONC	3.0 ± 0.1	19.5	1.12×10^{-5}	15.5
C87A/C104A-ONC	2.1 ± 0.1	32.0	2.62×10^{-5}	16.1

[a] Thermodynamic parameters were determined from GdnHCl-induced transition curves at pH 5.5 as described in Materials and Methods. $\Delta\Delta G^{[D]_{50\%}}$ is the difference in free energy between wt-ONC and an ONC variant at the transition midpoint of the respective variant. Parameters of unfolding were calculated from the rate constants presented in Figure 4 as described in Materials and Methods. $\Delta\Delta G_U^{\ddagger[D]_{50\%}}$ is the difference in free energy of activation between wt-ONC and an ONC variant at the transition midpoint of the respective variant.

of the C-terminal disulfide bond decreased T_m most considerably by 19 K.

GdnHCl-Induced Denaturation. To study the effect of the mutations on the thermodynamic stability of the ONC molecule, GdnHCl-induced transition curves were recorded (Figure 3). With a ΔG^{H_2O} value of 61.1 ± 3.1 kJ mol^{-1} wt-ONC was more stable than any of the variants investigated. The values of $[D]_{50\%}$ and the change in standard free energy at the transition midpoint ($\Delta\Delta G^{[D]_{50\%}}$) are summarized in Table 2.

The order of the degree of destabilization as the result of the amino acid substitutions was the same as for the temperature-induced unfolding. Modifications of the N-terminal pyroglutamate had the smallest impact on the thermodynamic stability. Amino acid substitutions in the hydrophobic cluster resulted in a strong destabilization of the ONC molecule by 1.4−1.6 M GdnHCl. Again, the substitution of the unique Phe28 by either Thr or Ala resulted in a slightly more pronounced destabilization than the substitution of the conserved Phe36 by Tyr. With a transition midpoint at 2.1 M GdnHCl, C87A/C104A-ONC proved to be the least stable variant.

Folding Experiments. The decreased thermodynamic stability of the ONC variants could arise from a faster unfolding or slower refolding (or both). To dissect the effect of the mutations, rate constants of unfolding and refolding of wt-ONC and its variants were determined with GdnHCl as denaturant (Figure 4).

Rate constants of the unfolding and refolding reaction were determined by fluorescence measurements at 20 °C. Because ONC possesses only one Trp residue but six Phe residues, the kinetics were followed at three different wavelengths to disclose possible local differences in the processes. The progress curves followed first-order kinetics over the entire range of conditions, and the detection at all three wavelengths yielded the same rate constants. Except for C87A/C104A-ONC, the refolding of the ONC variants is indistinguishable from that of wt-ONC. In contrast, the unfolding reaction of these variants is more or less strongly affected by the mutations. From the values of k_U at the respective transition midpoint (Table 2), values of $\Delta G_U^{\ddagger[D]_{50\%}}$ and $\Delta\Delta G_U^{\ddagger[D]_{50\%}}$

were calculated (Table 2). The correspondence of the values for $\Delta\Delta G_U^{\ddagger[D]_{50\%}}$ and $\Delta\Delta G^{[D]_{50\%}}$ (Table 2) clearly indicates that the thermodynamic destabilization of the variants has to be attributed to a destabilization of the native state. However, for C87A/C104A-ONC both the unfolding reaction and the refolding reaction are impaired by the deletion of the disulfide bond. Consequently, $\Delta\Delta G_U^{\ddagger[D]_{50\%}}$ and $\Delta\Delta G^{[D]_{50\%}}$ clearly differ, but the difference is covered by $\Delta\Delta G_f^{\ddagger[D]_{50\%}}$ (16.1 kJ mol^{-1}) as calculated from the values of k_f (1.70×10^{-5} s^{-1} for wt-ONC, 2.54×10^{-7} s^{-1} for C87A/C104A-ONC) at the transition midpoint of C87A/C104A-ONC.

DISCUSSION

Onconase is not only a potent antitumor therapeutic (*32*, *33*), but it had been shown to be unusually stable although originating from a mesophilic source (*3*, *9*−*11*, *16*, *17*). A comparison of the primary and tertiary structure of ONC with RNase A, which is the principal member of the RNase A superfamily, does not divulge an obvious basis for the increase of T_m from 60.4 °C (*34*) to 88.5 °C, of the value of $[GdnHCl]_{1/2}$ from 2.8 M (*19*) to 4.4 M, and of the value of ΔG^{H_2O} from 38 kJ mol^{-1} (*19*) to about 60 kJ mol^{-1}. Despite these studies concerning the thermodynamic stability and the fact that RNase A has been an intensively studied model protein of folding/unfolding processes for decades (*35*), the folding and unfolding of its homologue, ONC, and mutants thereof are described here for the first time.

An increased thermodynamic stability could be caused by a faster folding or a slower unfolding (or both) (*36*). The comparison of the chevron plot for wt-ONC (Figure 4) with the corresponding data for RNase A (*37*) clearly reveals an almost unchanged folding branch of the rate constants whereas the unfolding branches dramatically differ as a consequence of an ∼1000-fold slower unfolding reaction of ONC. These results could explain the high proteolytic stability of ONC (*17*) because unfolding in vivo is followed by irreversible processes such as proteolytic degradation (*38*).

The investigation of mutant variants of ONC was expected to shed light on the structural basis for the differences in the thermodynamic and kinetic stability. Despite the lack of regular interactions, loops can play an important role in folding or unfolding reactions (*39*) as had been shown for RNase A (*40*). In fact, the loops in ONC are shorter than in RNase A (*7*), which might be a reason for the increased stiffness of ONC (*41*). Also, the primary structure of the two proteins differs most significantly in the loop regions. The analysis of the number of interactions in the loops, however, reveals no significant increase for ONC (*7*).

The contribution of the chain termini to the activity and stability of ONC has been widely investigated by site-directed mutagenesis. These results are here expanded by the analysis of folding/unfolding kinetics. The decreased activity of variants lacking the cyclized pyroglutamate structure at the N-terminus obviously results from a loss of a hydrogen bond between the 5-oxo group of pyroglutamate and Lys9. The values determined for <E1E- and <E1P-ONC in this paper agree with those for a <E1E variant of the homologue from *Rana catesbeiana*, which showed 28% residual activity (*42*), and <E1A-ONC, which showed 57% residual activity (*11*). The coincidence of the values for <E1E- and <E1P-ONC, which cannot form a hydrogen bond to the side chain of Lys9, indicates that also glutamate in position 1 obviously is not able to form that hydrogen bond.

With a decrease of T_m by 1−2 K or of $[GdnHCl]_{50\%}$ by 0.3−0.5 M GdnHCl, the impact of mutations of <E1 on the stability of the ONC molecule is rather small (Tables 1 and 2). Notomista et al. (*9*) have speculated that the loss of the hydrogen bond and, thus, the tether of the N-terminus to the protein body might be counterbalanced by the extension of helix I. Also, the solution structure of <E1S-ONC did not show any increased flexibility of the N-terminus in comparison to wt-ONC, indicating the maintenance of the native structure (*43*). The present folding and unfolding experiments with <E1E- and <E1P-ONC clearly reveal that the thermodynamic destabilization of these variants has to be attributed to a faster unfolding reaction (Figure 4, Table 2) pointing to an impact of these amino acid substitutions on the native state only.

The deletion of the C-terminal disulfide bond dramatically decreases the transition temperature by about 20 K (Table 1) and impairs the thermodynamic stability by more than 30 kJ mol^{-1} (Table 2) whereas the catalytic activity decreases only moderately to 66% (Table 1). These data coincide well with the values determined by Leland et al. (*10*), and similar results were obtained for C87S/Δ104- and C87S/Δ103−104-ONC variants (*9*). The corresponding C-terminal portion of RNase A had been shown to be crucial for the folding reaction (*31*, *44*), and T_m of the RNase A molecule was increased by about 5 K by the introduction of a new disulfide bond that links the N- and C-terminus (A4C/V118C-RNase A) (*45*). A stabilizing effect of disulfide bonds is commonly attributed to a restriction of the conformational freedom of the unfolded state and, thus, to an increased folding rate, but effects on the native state of proteins have also been described (*46*). The chevron plot (Figure 4) clearly shows a decreased folding as well as an increased unfolding rate constant for C87A/C104A-ONC compared to wt-ONC. As for the decreased folding rate, it is feasible that the 87−104 disulfide bond not only decreases the entropy of the polypeptide chain in the unfolded state but also facilitates the formation of the native structure of the C-terminus in wt-ONC which is impeded in the C87A/C104A-ONC variant. From the ratio $\Delta\Delta G_U^{\ddagger[D]_{50\%}}$ to $\Delta\Delta G_f^{\ddagger[D]_{50\%}}$, however, half of the thermodynamic destabilization has to be attributed to a faster unfolding of this variant; i.e., also the native state is affected by the deletion. The crystal structures of wt-ONC and C87S/Δ103−104-ONC, on the other hand, are "extremely close" (*41*), which is supported by MD simulations at 300 K. In contrast, at 350 K the mutant protein shows stronger overall fluctuations as does wt-ONC (*41*). Whether the deletion of the covalent tether finally even alters the folding or unfolding pathways of the ONC molecule remains unsolved with data presented here and will be shown by future studies.

Special attention was paid to the contribution of the hydrophobic cluster to the stability of the ONC molecule. This cluster had been shown to be of exceeding importance for the stability of RNase A (*13*, *47*) and was proposed as the initiation site of unfolding in RNase A (*13*, *30*). The replacement of Met23 in the corresponding cluster in ONC by leucine had been reported to decrease the thermodynamic stability by about 12 kJ mol^{-1} (*17*). Replacement of the fully

buried core residue Phe36 (corresponding to Phe46 in RNase A) by tyrosine resulted in a dramatic decrease of T_m by 9.3 K and of $\Delta\Delta G^{[D]_{50\%}}$ by 19.5 kJ mol^{-1}, corresponding to a loss of 32% of the thermodynamic stability. The respective amino acid substitution in RNase A resulted in a ΔT_m of 9.0 K and $\Delta\Delta G^{[D]_{50\%}}$ of 10.8 kJ mol^{-1}, corresponding to 28% of the thermodynamic stability (*13*). Interestingly, the replacement of Phe28, which extends the hydrophobic cluster in ONC but is Thr in most of the other members of the RNase A superfamiliy, destabilizes the ONC molecule to an even larger extent (Tables 1 and 2, Figures 3 and 4) regardless of its substitution by Thr or Ala. The decreased thermodynamic stability of all these variants can be attributed to a faster unfolding reaction only in comparison to wt-ONC. The removal of the covalent disulfide bond results in a stronger thermodynamic destabilization of the ONC molecule than the deletion of the additional hydrophobic interaction by Phe28. However, the impact on the unfolding reaction is significantly more severe for Phe28, emphasizing the central importance of this residue for the maintenance of the native conformation of the ONC molecule.

An additional structural difference between ONC and other members of the RNase A superfamily is the occurrence and number of *cis*-peptidyl proline bonds. *cis*-Peptidyl proline bonds, which make 5.2% of all peptidyl proline bonds in folded proteins (*48*), generate points of structural instability because the unfolded state favors the *trans* configuration (*49*). Consequently, proteins lacking *cis*-prolines should be more stable than their *cis*-proline-containing homologues. Interestingly, ONC contains only *trans*-prolines whereas RNase A (30% sequence identity) contains two *cis*-prolines and is less stable than ONC by about 30 °C. The sialic acid binding proteins from the frogs *R. catesbeiana* (53% sequence identity) and *Rana japonica* (48% sequence identity), both of which possess one *cis*-proline (Pro80), are less stable than ONC by more than 15 K (*50*). Amino acid substitutions for *cis*-prolines, however, usually fail to stabilize the protein structure because the *cis* configuration is even far less favorable for non-proline peptide bonds (*51*). Accordingly, only 0.03% of non-proline peptide bonds occur in the *cis* configuration in folded proteins (*52*). A way to stabilize *cis*-proline-containing proteins or protein regions is the introduction of mimics or proline analogues that are conformationally restricted and, thus, no longer can adopt the *trans* configuration, e.g., 5,5-dimethylproline (*44*, *53*). Consequently, it would be interesting to analyze the folding/unfolding behavior of the ONC homologues from *R. catesbeiana* and *R. japonica* containing conformationally restricted proline analogues.

In summary, the structural peculiarities of ONC such as the N-terminal pyroglutamate residue, the C-terminal disulfide bond, and the central hydrophobic cluster yield distinct contributions to the high stability of this protein. In comparison to RNase A, the stabilization is mainly caused by a strongly decreased unfolding rate constant. Among the determinants of unfolding, the unique Phe28 residue has the greatest importance.

ACKNOWLEDGMENT

The authors thank Professor R. T. Raines (University of Wisconsin—Madison, WI) for the gift of the plasmids encoding for wild-type and C87A/C104A-ONC and Dr. A. Schierhorn (Martin-Luther University Halle-Wittenberg, Germany) for performing mass spectrometry measurements.

SUPPORTING INFORMATION AVAILABLE

Oligonucleotide sequences for the site-directed mutagenesis and PCR reactions. This material is available free of charge via the Internet at http://pubs.acs.org.

REFERENCES

1. Darzynkiewicz, Z., Carter, S. P., Mikulski, S. M., Ardelt, W. J., and Shogen, K. (1988) Cytostatic and cytotoxic effects of Pannon (P-30 protein), a novel anticancer agent, *Cell Tissue Kinet. 21*, 169−182.
2. Juan, G., Ardelt, B., Li, X., Mikulski, S. M., Shogen, K., Ardelt, W., Mittelman, A., and Darzynkiewicz, Z. (1998) G1 arrest of U937 cells by onconase is associated with suppression of cyclin D3 expression, induction of p16INK4A, p21WAF1/CIP1 and p27KIP and decreased pRb phosphorylation, *Leukemia 12*, 1241−1248.
3. Leland, P. A., Schultz, L. W., Kim, B. M., and Raines, R. T. (1998) Ribonuclease A variants with potent cytotoxic activity, *Proc. Natl. Acad. Sci. U.S.A. 95*, 10407−10412.
4. Eijsink, V. G., Bjork, A., Gaseidnes, S., Sirevag, R., Synstad, B., van den Burg, B., and Vriend, G. (2004) Rational engineering of enzyme stability, *J. Biotechnol. 113*, 105−120.
5. Berezovsky, I. N., and Shakhnovich, E. I. (2005) Physics and evolution of thermophilic adaptation, *Proc. Natl. Acad. Sci. U.S.A. 102*, 12742−12747.
6. Sadeghi, M., Naderi-Manesh, H., Zarrabi, M., and Ranjbar, B. (2006) Effective factors in thermostability of thermophilic proteins, *Biophys. Chem. 119*, 256−270.
7. Mosimann, S. C., Ardelt, W., and James, M. N. (1994) Refined 1.7 Å X-ray crystallographic structure of P-30 protein, an amphibian ribonuclease with anti-tumor activity, *J. Mol. Biol. 236*, 1141−1153.
8. Kolbanovskaya, E. Y., Terwisscha van Scheltinga, A. C., Mukhortov, V. G., Ardelt, W., Beintema, J. J., and Karpeisky, M. Y. (2000) Localization and analysis of nonpolar regions in onconase, *Cell. Mol. Life Sci. 57*, 1306−1316.
9. Notomista, E., Catanzano, F., Graziano, G., Di Gaetano, S., Barone, G., and Di Donato, A. (2001) Contribution of chain termini to the conformational stability and biological activity of onconase, *Biochemistry 40*, 9097−9103.
10. Leland, P. A., Staniszewski, K. E., Kim, B., and Raines, R. T. (2000) A synapomorphic disulfide bond is critical for the conformational stability and cytotoxicity of an amphibian ribonuclease, *FEBS Lett. 477*, 203−207.
11. Liao, Y. D., Wang, S. C., Leu, Y. J., Wang, C. F., Chang, S. T., Hong, Y. T., Pan, Y. R., and Chen, C. (2003) The structural integrity exerted by N-terminal pyroglutamate is crucial for the cytotoxicity of frog ribonuclease from *Rana pipiens*, *Nucleic Acids Res. 31*, 5247−5255.
12. Beintema, J. J., Breukelman, H. J., Carsana, A., and Furia, A. (1997) Evolution of vertebrate ribonucleases: ribonuclease A superfamily, in *Ribonucleases: Structures and Functions* (D'Alessio, G., and Riordan, J. F., Eds.) pp 245−269, Academic Press, New York.
13. Köditz, J., Ulbrich-Hofmann, R., and Arnold, U. (2004) Probing the unfolding region of ribonuclease A by site-directed mutagenesis, *Eur. J. Biochem. 271*, 4147−4156.
14. Boix, E., Wu, Y., Vasandani, V. M., Saxena, S. K., Ardelt, W., Ladner, J., and Youle, R. J. (1996) Role of the N terminus in RNase A homologues: differences in catalytic activity, ribonuclease inhibitor interaction and cytotoxicity, *J. Mol. Biol. 257*, 992−1007.
15. Newton, D. L., Boque, L., Wlodawer, A., Huang, C. Y., and Rybak, S. M. (1998) Single amino acid substitutions at the N-terminus of a recombinant cytotoxic ribonuclease markedly influence biochemical and biological properties, *Biochemistry 37*, 5173−5183.
16. Lee, J. E., and Raines, R. T. (2003) Contribution of active-site residues to the function of onconase, a ribonuclease with antitumoral activity, *Biochemistry 42*, 11443−11450.

17. Notomista, E., Catanzano, F., Graziano, G., Dal Piaz, F., Barone, G., D'Alessio, G., and Di Donato, A. (2000) Onconase: an unusually stable protein, *Biochemistry 39*, 8711−8718.
18. Sanger, F., Nicklen, S., and Coulson, A. R. (1977) DNA sequencing with chain-terminating inhibitors, *Proc. Natl. Acad. Sci. U.S.A. 74*, 5463−5467.
19. Markert, Y., Köditz, J., Ulbrich-Hofmann, R., and Arnold, U. (2003) Proline versus charge concept for protein stabilization against proteolytic attack, *Protein Eng. 16*, 1041−1046.
20. Arnold, U., Hinderaker, M. P., Nilsson, B. L., Huck, B. R., Gellman, S. H., and Raines, R. T. (2002) Protein prosthesis: a semisynthetic enzyme with a beta-peptide reverse turn, *J. Am. Chem. Soc. 124*, 8522−8523.
21. Pace, C. N., Vajdos, F., Fee, L., Grimsley, G., and Gray, T. (1995) How to measure and predict the molar absorption coefficient of a protein, *Protein Sci. 4*, 2411−2423.
22. Corbishley, T. P., Johnson, P. J., and Williams, R. (1984) Serum ribonucleases, in *Methods of enzymatic catalysis* (Bergmeyer, H. U., Ed.) pp 134−143, VCH, Weinheim.
23. Sambrook, J., Fritsch, E. F., and Maniatis, T. (1989) *Molecular cloning: a laboratory manual*, Cold Spring Harbor Laboratory, Cold Spring Harbor, NY.
24. Curtis, P. J., Burdon, M. G., and Smellie, R. M. (1966) The purification from rat liver of a nuclease hydrolysing ribonucleic acid and deoxyribonucleic acid, *Biochem. J. 98*, 813−817.
25. Santoro, M. M., and Bolen, D. W. (1988) Unfolding free energy changes determined by the linear extrapolation method. 1. Unfolding of phenylmethanesulfonyl alpha-chymotrypsin using different denaturants, *Biochemistry 27*, 8063−8068.
26. Clarke, J., and Fersht, A. R. (1993) Engineered disulfide bonds as probes of the folding pathway of barnase: increasing the stability of proteins against the rate of denaturation, *Biochemistry 32*, 4322−4329.
27. Pace, C. N. (1986) Determination and analysis of urea and guanidine hydrochloride denaturation curves, in *Methods in Enzymology* (Hirs, C. H. W., and Timasheff, S. N., Eds.) pp 266−280, Academic Press, New York.
28. Maxwell, K. L., Wildes, D., Zarrine-Afsar, A., De Los Rios, M. A., Brown, A. G., Friel, C. T., Hedberg, L., Horng, J. C., Bona, D., Miller, E. J., Vallee-Belisle, A., Main, E. R., Bemporad, F., Qiu, L., Teilum, K., Vu, N. D., Edwards, A. M., Ruczinski, I., Poulsen, F. M., Kragelund, B. B., Michnick, S. W., Chiti, F., Bai, Y., Hagen, S. J., Serrano, L., Oliveberg, M., Raleigh, D. P., Wittung-Stafshede, P., Radford, S. E., Jackson, S. E., Sosnick, T. R., Marqusee, S., Davidson, A. R., and Plaxco, K. W. (2005) Protein folding: defining a "standard" set of experimental conditions and a preliminary kinetic data set of two-state proteins, *Protein Sci. 14*, 602−616.
29. Laemmli, U. K. (1970) Cleavage of structural proteins during the assembly of the head of bacteriophage T4, *Nature 227*, 680−685.
30. Arnold, U., Rücknagel, K. P., Schierhorn, A., and Ulbrich-Hofmann, R. (1996) Thermal unfolding and proteolytic susceptibility of ribonuclease A, *Eur. J. Biochem. 237*, 862−869.
31. Bhat, R., Wedemeyer, W. J., and Scheraga, H. A. (2003) Proline isomerization in bovine pancreatic ribonuclease A. 2. Folding conditions, *Biochemistry 42*, 5722−5728.
32. Mikulski, S. M., Costanzi, J. J., Vogelzang, N. J., McCachren, S., Taub, R. N., Chun, H., Mittelman, A., Panella, T., Puccio, C., Fine, R., and Shogen, K. (2002) Phase II trial of a single weekly intravenous dose of ranpirnase in patients with unresectable malignant mesothelioma, *J. Clin. Oncol. 20*, 274−281.
33. Vogelzang, N. J., Porta, C., and Mutti, L. (2005) New agents in the management of advanced mesothelioma, *Semin. Oncol. 32*, 336−350.
34. Arnold, U., and Ulbrich-Hofmann, R. (1997) Kinetic and thermodynamic thermal stabilities of ribonuclease A and ribonuclease B, *Biochemistry 36*, 2166−2172.
35. Raines, R. T. (1998) Ribonuclease A, *Chem. Rev. 98*, 1045−1066.
36. Fersht, A. R., Matouschek, A., and Serrano, L. (1992) The folding of an enzyme. I. Theory of protein engineering analysis of stability and pathway of protein folding, *J. Mol. Biol. 224*, 771−782.
37. Lin, S. H., Konishi, Y., Nall, B. T., and Scheraga, H. A. (1985) Influence of an extrinsic cross-link on the folding pathway of ribonuclease A. Kinetics of folding-unfolding, *Biochemistry 24*, 2680−2686.
38. Plaza del Pino, I. M., Ibarra-Molero, B., and Sanchez-Ruiz, J. M. (2000) Lower kinetic limit to protein thermal stability: a proposal regarding protein stability in vivo and its relation with misfolding diseases, *Proteins 40*, 58−70.
39. Fetrow, J. S. (1995) Omega loops: nonregular secondary structures significant in protein function and stability, *FASEB J. 9*, 708−717.
40. Arnold, U., Köditz, J., Markert, Y., and Ulbrich-Hofmann, R. (2005) Local fluctuations vs. global unfolding of proteins investigated by limited proteolysis, *Biocatal. Biotransfor. 23*, 159−167.
41. Merlino, A., Mazzarella, L., Carannante, A., Fiore, A. D., Donato, A. D., Notomista, E., and Sica, F. (2005) The importance of dynamic effects on the enzyme activity: X-ray structure and molecular dynamics of onconase mutants, *J. Biol. Chem. 280*, 17953−17960.
42. Leu, Y. J., Chern, S. S., Wang, S. C., Hsiao, Y. Y., Amiraslanov, I., Liaw, Y. C., and Liao, Y. D. (2003) Residues involved in the catalysis, base specificity, and cytotoxicity of ribonuclease from *Rana catesbeiana* based upon mutagenesis and X-ray crystallography, *J. Biol. Chem. 278*, 7300−7309.
43. Gorbatyuk, V. Y., Tsai, C. K., Chang, C. F., and Huang, T. H. (2004) Effect of N-terminal and Met23 mutations on the structure and dynamics of onconase, *J. Biol. Chem. 279*, 5772−5780.
44. Arnold, U., Hinderaker, M. P., Köditz, J., Golbik, R., Ulbrich-Hofmann, R., and Raines, R. T. (2003) Protein prosthesis: a nonnatural residue accelerates folding and increases stability, *J. Am. Chem. Soc. 125*, 7500−7501.
45. Klink, T. A., and Raines, R. T. (2000) Conformational stability is a determinant of ribonuclease A cytotoxicity, *J. Biol. Chem. 275*, 17463−17467.
46. Hinck, A. P., Truckses, D. M., and Markley, J. L. (1996) Engineered disulfide bonds in staphylococcal nuclease: effects on the stability and conformation of the folded protein, *Biochemistry 35*, 10328−10338.
47. Kadonosono, T., Chatani, E., Hayashi, R., Moriyama, H., and Ueki, T. (2003) Minimization of cavity size ensures protein stability and folding: structures of Phe46-replaced bovine pancreatic RNase A, *Biochemistry 42*, 10651−10658.
48. MacArthur, M. W., and Thornton, J. M. (1991) Influence of proline residues on protein conformation, *J. Mol. Biol. 218*, 397−412.
49. Osvath, S., and Gruebele, M. (2003) Proline can have opposite effects on fast and slow protein folding phases, *Biophys. J. 85*, 1215−1222.
50. Okabe, Y., Katayama, N., Iwama, M., Watanabe, H., Ohgi, K., Irie, M., Nitta, K., Kawauchi, H., Takayanagi, Y., Oyama, F., et al. (1991) Comparative base specificity, stability, and lectin activity of two lectins from eggs of *Rana catesbeiana* and *R. japonica* and liver ribonuclease from *R. catesbeiana*, *J. Biochem. 109*, 786−790.
51. Schultz, D. A., and Baldwin, R. L. (1992) Cis proline mutants of ribonuclease A. I. Thermal stability, *Protein Sci. 1*, 910−916.
52. Stewart, D. E., Sarkar, A., and Wampler, J. E. (1990) Occurrence and role of cis peptide bonds in protein structures, *J. Mol. Biol. 214*, 253−260.
53. An, S. S. A., Cathy, C. C., Peng, J.-L., Li, Y.-J., Rothwarf, D. M., Welker, E., Thannhauser, T. W., Zhang, L. S., Tam, J. P., and Scheraga, H. A. (1999) Retention of the cis proline conformation in tripeptide fragments of bovine pancreatic ribonuclease A containing a non-natural proline analogue, 5,5-dimethylproline, *J. Am. Chem. Soc. 121*, 11558−11566.

BI0525223